THE ASTROPHYSICAL JOURNAL, 512:L35–L38, 1999 February 10

THE KILOHERTZ QPO FREQUENCY AND FLUX DECREASE IN AQUILA X-1 AND THE EFFECT OF SOFT X-RAY SPECTRAL COMPONENTS

W. YU,[1] T. P. LI,[1] W. ZHANG,[2] AND S. N. ZHANG[3,4]

Received 1998 September 16; accepted 1998 December 14; published 1999 January 13

ABSTRACT

We report on a *Rossi X-Ray Timing Explorer* observation of Aquila X-1 during its outburst in 1997 March in which, immediately following a type I burst, the broadband 2–10 keV flux decreased by about 10% and the kilohertz quasi-periodic oscillation (kHz QPO) frequency decreased from 813 ± 3 to 776 ± 4 Hz. This change in kHz QPO frequency is much larger than expected from a simple extrapolation of a frequency-flux correlation that was established in data before the burst. Meanwhile, a very low frequency noise component in the broadband fast Fourier transform power spectra, with a fractional rms amplitude of 1.2% before the burst, ceased to exist after the burst. All these changes were accompanied by a change in the energy spectral shape. If we characterize the energy spectra with a model composed of two blackbody (BB) components and a power-law component, almost all the decrease in flux was in the two BB components. We attribute the two BB components to the contributions from a region very near the neutron star, or even from the neutron star itself, and from the accretion disk, respectively.

Subject headings: stars: individual (Aquila X-1) — stars: neutron — X-rays: stars

1. INTRODUCTION

Kilohertz quasi-periodic oscillations (kHz QPOs) have been observed in about 20 low-mass X-ray binaries (LMXBs) by the *Rossi X-Ray Timing Explorer* (*RXTE*) since its launch at the end of 1995 (van der Klis 1998). Although the detailed production mechanism of these QPOs is not fully understood, there is little doubt that they correspond to the dynamical timescale near the neutron star surface, and as such they enable us to probe strong gravity effects and the equation of state of neutron stars (Kaaret, Ford, & Chen 1997; Zhang et al. 1996; van der Klis 1998; Miller & Lamb 1998; Lamb, Miller, & Psaltis 1998).

The kHz QPO frequency has been found to correlate with at least two quantities: the source count rate or flux and the energy spectral shape or hardness ratios (van der Klis 1998 and references therein; Kaaret et al. 1998; Zhang et al. 1998c; Méndez et al. 1999). Soft X-ray transients like 4U 1608−52 and Aql X-1, with their large swings in both count rates and energy spectral shapes, are ideal for the study of these kinds of correlations. Both 4U 1608−52 and Aql X-1 have been observed with the *RXTE* Proportional Counter Array (PCA) during their outburst decay. A similar correlation between the QPO frequency and the X-ray flux has been observed in different flux ranges (Yu et al. 1997; Méndez et al. 1998; Zhang et al. 1998b). In each flux range, the QPO frequency appears correlated with the X-ray flux. Spectral studies suggest that there is a significant correlation between the QPO frequency and the spectral shape, even among data from different flux ranges in 4U 1608−52 (Kaaret et al. 1998). A correlation between the QPO frequency and the spectral shape has also been found in other QPO sources. For example, a correlation between the QPO frequency and the flux of the blackbody component was observed in 4U 0614+091 (Ford et al. 1997).

The QPO frequency is usually regarded as the Keplerian frequency at the inner disk radius or its beat frequency with the neutron star spin in the beat-frequency model (Alpar & Shaham 1985; Lamb et al. 1985; Strohmayer et al. 1996; Zhang, Yu, & Zhang 1998a; Miller, Lamb, & Psaltis 1998). The higher the mass accretion rate, the higher should be the QPO frequency. This will lead to a correlation between the QPO frequency and the flux. However, when a transition of the accretion state happens, the same mass accretion rate may correspond to different inner disk radii and different fluxes before and after the transition. A spectral variation is probably associated with a variation of the accretion state and might lead to a new flux range or frequency range. A comparison of the spectral components before and after the spectral variation and a study of the correlation between QPO frequency and the spectral shape will help to reveal how the kHz QPOs are generated. In this Letter, we present our study with the *RXTE*/PCA data before and after an X-ray burst in Aql X-1.

2. OBSERVATIONS AND DATA ANALYSIS

An X-ray burst with a peak PCA count rate about 40,000 counts s^{-1} was observed by the *RXTE* PCA on 1997 March 1, when the daily-averaged all-sky monitor (ASM) count rate is ~4 counts s^{-1}. Nearly coherent oscillation at about 549 Hz was detected in the X-ray burst. An ~10% flux decrease and a corresponding QPO frequency decrease were observed after the X-ray burst (Zhang et al. 1998b). The count rate decrease is ~64 counts s^{-1} in the entire PCA band. The data used for timing analysis in the kHz frequency range are taken in the event mode "E_125us_64M_0_1s." The energy range of 2–10 keV was selected, the same as those used in Zhang et al. (1998b). The Standard 1 data are used to study the frequency range below 0.5 Hz. The Standard 2 data are used in the spectral analysis. All the errors quoted in the following are 1 σ errors. The low-energy response of the *RXTE*/PCA detectors is not sufficient in constraining the absorption column density N_H. We have fixed it at 3.0×10^{21} cm^{-2} in our spectral fittings, ac-

[1] Laboratory for Cosmic Ray and High Energy Astrophysics, Institute of High Energy Physics, Chinese Academy of Sciences, P.O. Box 918-3, Beijing, 100039, China.

[2] Laboratory for High Energy Astrophysics, NASA/Goddard Space Flight Center, Greenbelt, MD 20771.

[3] University of Alabama in Huntsville, Department of Physics, Huntsville, AL 35899.

[4] NASA/Marshall Space Flight Center, ES-84, Huntsville, AL 35812.

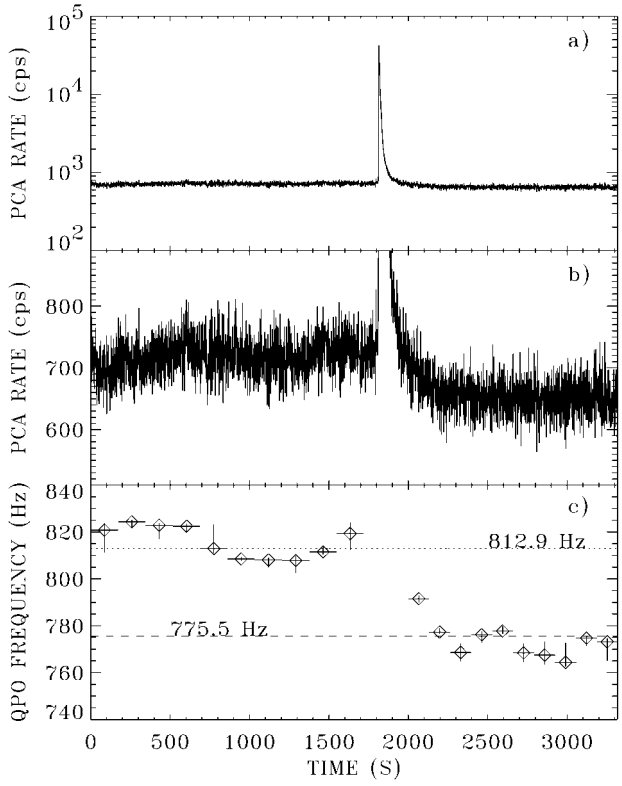

FIG. 1.—Light curve and the kHz QPO evolution around the X-ray burst. (*a*) The light curve in the entire PCA energy band (~2–60 keV) with background subtraction; (*b*) the flux decrease shown in detail; (*c*) the QPO frequency evolution around the burst.

cording to previous studies (Czerny, Czerny, & Grindlay 1987; Verbunt et al. 1994; Zhang et al. 1998a).

2.1. *Timing Analysis*

We first calculate the dynamical power spectra around the X-ray burst. Then a model composed of a constant and a Lorentzian function is fitted to the 200–2000 Hz power spectra in order to determine the QPO frequency. In Figure 1, we show the light curve around the X-ray burst and how QPO frequency evolved. The QPO frequency decreased from about 813 ± 3 Hz before the burst to 776 ± 4 Hz after the burst. In Figure 2, the QPO frequency versus PCA count rate (CR) in the energy range of 2–10 keV is shown for the observation of two consecutive *RXTE* orbits on March 1. The data points in the lower left-hand corner are taken after the X-ray burst, and those points on the right-hand side branch are taken before the X-ray burst. We apply a linear model in order to fit the right-hand side branch, and we get $f_{\rm qpo} = -(219.4 \pm 32.0) + (1.954 \pm 0.002) \times {\rm CR}$. The average count rate after the X-ray burst in the 2–10 keV band is ~478 counts s^{-1}; the inferred QPO frequency from the above QPO frequency versus count rate relation at this count rate is 714 ± 30 Hz. Thus, the inferred QPO frequency decrease is about 99 ± 30 Hz, which is more than twice the observed frequency decrease of 37 ± 5 Hz.

In order to study the source variability at frequencies lower than 0.5 Hz, we divide the light curve into 256 s segments and then calculate the power spectrum of each segment. We average 16 power spectra before the X-ray burst and four power spectra after the burst. In Figure 3, we show the average Leahy normalized power spectra in the frequency range of 0.002–0.5 Hz

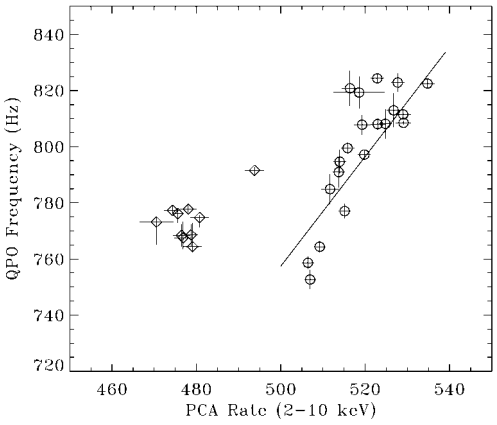

FIG. 2.—The kHz QPO frequency vs. PCA count rate (2–10 keV) relation observed on March 1. The data points on the left (*diamonds*) are taken after the X-ray burst, and those on the right (*circles*) are taken before the burst.

before and after the X-ray burst. The power spectrum before the X-ray burst shows a very low frequency noise (VLFN) component of a power-law form (Hasinger & van der Klis 1989). A model composed of a white noise level of 2 and a power-law component is fitted to the average power spectra. We obtain a power-law index $\alpha = 1.5 \pm 0.2$ and $A = 0.0024 \pm 0.0015$. The fractional rms variability of the VLFN is about 1.2% ± 0.4%. The power spectrum after the X-ray burst is consistent with the white noise.

2.2. *Spectral Analysis*

The energy spectrum of Aql X-1 has changed little during the outburst before March 1 (Zhang et al. 1998b) and was of a blackbody type. In subsequent observations, the energy spectra gradually changed from a blackbody type to a blackbody plus a power-law type (see Zhang et al. 1998a). The spectra before and after the X-ray burst are shown in Figure 4. In Figure 4*a*, we plot the ratio between the spectra (2–10 keV) before and after the X-ray burst, namely, spectrum $N_1(E)$ and spectrum $N_2(E)$, respectively. The ratio as a function of energy is not a constant. The flux decrease is more severe above 5

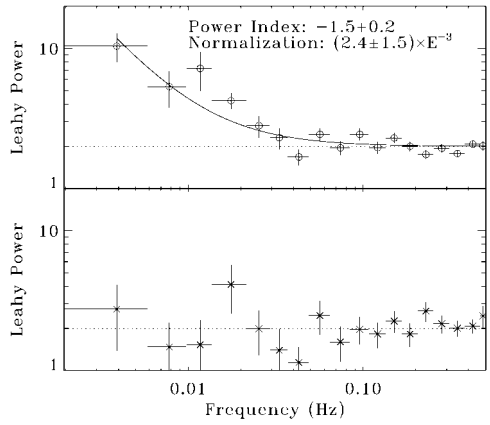

FIG. 3.—The power spectra (0.002–0.5 Hz) for the entire PCA band before and after the X-ray burst. The upper panel and the lower panel correspond to data before and after the X-ray burst, respectively. The power spectrum in the upper panel shows a VLFN component, while the power spectrum in the lower panel agrees with the white noise. The best-fit model, composed of a constant white noise level of 2 and a power-law VLFN, is shown in the upper panel.

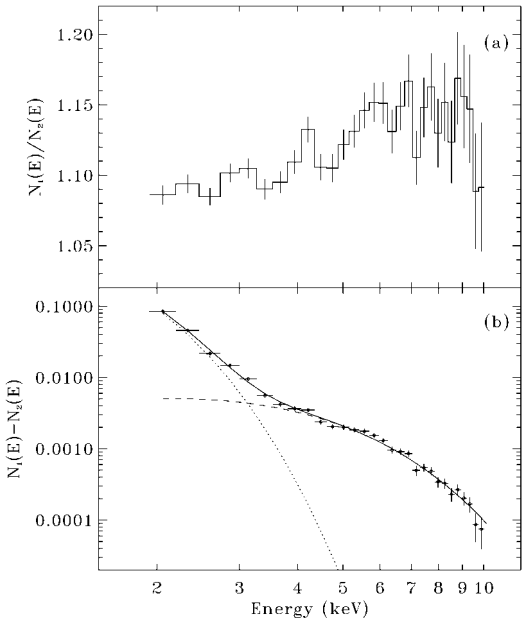

FIG. 4.—Comparison of the energy spectra before the X-ray burst, $N_1(E)$, and after the X-ray burst, $N_2(E)$, in the energy range of 2–10 keV. (*a*) Ratio of the two spectra $[N_1(E)/N_2(E)]$; (*b*) difference between the two spectra $[N_1(E) - N_2(E)]$ in units of photons cm^{-2} keV^{-1} s^{-1} (see Table 2). The model (*solid line*), the 0.28 keV component (*dotted line*), and the 1.15 keV component (*dashed line*) are also shown.

keV. Thus, a variation of the spectral shape was associated with the flux decrease.

Spectral models of a single blackbody (BB), a single power law (PL), and their combination (BB + PL) cannot yield an acceptable fit to both spectra $N_1(E)$ and $N_2(E)$ in the energy range of 3–20 keV. The model composed of two BB components and a PL component gives an acceptable fit. The inclusion of two BB components, one of which may be a multicolor disk (MCD) component, has been applied previously to the soft X-ray transient 4U 1608−52 during an outburst (Mitsuda et al. 1984) and Aql X-1 during an outburst rise (Cui et al. 1998). In Table 1, we list the parameters of the spectral fit to both spectra with 2BB + PL and BB + MCD + PL models. The emission area of the ~0.26 keV BB component in the 2BB + PL model fit is much larger than the surface area of a neutron star. This suggests that it may be a disk component and that the fit with the BB + MCD + PL model may be reasonable. Assuming the disk inclination angle is zero, we find that the apparent inner disk radius is in the 1 σ range of 200–470 km. In both spectra, the PL components only contribute less than 1/20 of the total flux in the energy range of 2–10 keV. The difference between the average PCA count rate (>10 keV) before and after the X-ray burst is 0.64 ± 0.38 counts s^{-1}. This indicates that the PCA flux variation mainly comes from the spectral components in the soft X-ray range below 10 keV.

The two BB temperatures are stable during the flux decrease, as shown in Table 1. Thus, it is reasonable to study the flux decrease by subtracting the spectrum $N_2(E)$ from the spectrum $N_1(E)$. In Figure 4*b*, we plot the subtracted spectrum $[N_1(E) - N_2(E)]$ in the energy range of 2–10 keV. A model composed of two BB components yields an acceptable fit to this spectrum, which is also plotted. In Table 2, we list the best-fit parameters and the fluxes of the two components. The 2–10 keV energy flux of the residual spectrum is about 7% ± 2% that of the total before the X-ray burst. The subtraction of the PL components in Table 1 mainly affects the 0.28 keV component shown in Figure 4*b*, i.e., a flux of 0.7 ± 2.5 photons cm^{-2} s^{-1} in 2–4 keV.

3. DISCUSSION AND CONCLUSION

We have reported that there was a simultaneous decrease of the X-ray flux, the QPO frequency, and the VLFN component in Aql X-1 immediately following a type I X-ray burst. The decrease lasted at least 400 s until the observation was stopped. The flux decrease was mainly due to a decrease of the spectral components in the energy range below 10 keV. Since a type I X-ray burst only occurs when the condition for the thermonuclear instability is met, the X-ray burst and the flux decrease may be causally related.

The X-ray flux derived from the spectral fit in Table 1 has an uncertainty as large as 20%, which is insufficient to determine the decrease of the X-ray luminosity. However, the spectral fit shown in Table 2 yields more confined parameters, suggesting that there is a 7% ± 2% decrease of the X-ray luminosity in 2–10 keV. The index of the PL component decreases together with the decrease of the X-ray luminosity. This behavior is similar to that found in 4U 1608−52 and 4U 0614+091 (Kaaret et al. 1998).

The spectral parameters of the two BB components in Table 1 seem consistent with the trend shown in Figure 2 of Cui et al. (1998), i.e., the lower the ASM count rate of Aql X-1, the larger the inner disk radius and the lower the BB temperatures are. The ~1.06 keV BB is probably related to a part of the neutron star surface. The decrease of the VLFN after the burst supports the idea. The VLFN in LMXBs is an indication of the time-dependent fusion reactions (fires) on the neutron star surface (Bildsten 1993), which correspond to a

TABLE 1

PARAMETERS OF THE SPECTRA $N_1(E)$ AND $N_2(E)$ (3–20 keV)

Spectrum	Model	T_1,[a] T_{MCD}[b] (keV)	R_1,[c] N_{MCD}[d]	T_2[a] (keV)	R_2[c]	Index[e]	N_{PL}[f]	χ^2/dof
$N_1(E)$	2BB + PL	0.26 ± 0.01	274 ± 47	1.06 ± 0.01	2.09 ± 0.05	3.11 ± 0.13	0.37 ± 0.22	102.1/45
	BB + MCD + PL	0.28 ± 0.01	(9.0 ± 3.8) × 10^4	1.06 ± 0.01	2.09 ± 0.05	3.08 ± 0.13	0.32 ± 0.20	107.3/45
$N_2(E)$	2BB + PL	0.25 ± 0.01	326 ± 155	1.02 ± 0.01	2.14 ± 0.07	2.65 ± 0.14	0.15 ± 0.15	61.9/45
	BB + MCD + PL	0.27 ± 0.02	(1.3 ± 0.9) × 10^5	1.02 ± 0.01	2.13 ± 0.07	2.65 ± 0.15	0.16 ± 0.16	62.5/45

[a] BB temperature.
[b] The inner disk temperature in MCD.
[c] Apparent BB radii in units of kilometers, assuming that the distance to the source is 2.5 kpc.
[d] The normalization of disk BB in MCD: $[(R_{in}/\text{km})/(D/2.5\ \text{kpc})]^2 \cos(\theta)$, where R_{in} is the inner disk radius, D the distance to the source, and θ the angle of the disk.
[e] Photon spectral index.
[f] In units of photons cm^{-2} keV^{-1} s^{-1} at 1 keV.

TABLE 2

MODEL FIT TO THE SUBTRACTED SPECTRUM $N_1(E) - N_2(E)$ (2–10 keV)

T_1 (keV)	R_1[a] (km)	Flux1 (photons cm^{-2} s^{-1})	T_2 (keV)	R_2[a] (km)	Flux2 (photons cm^{-2} s^{-1})	χ^2/dof
0.28 ± 0.03	42 ± 12	(3.5 ± 1.4) × 10^{-2}	1.15 ± 0.03	0.62 ± 0.04	(1.5 ± 0.2) × 10^{-2}	31.0/25

[a] Apparent BB radii in units of kilometers for a distance of 2.5 kpc.

mass accretion rate larger than that of the bursting stage. The disappearance of the VLFN in Aql X-1 then not only suggests that at least a few percent of the observed X-ray flux was from the fusion reaction on the neutron star surface before the X-ray burst but also indicates that after the X-ray burst, the time-dependent fusion reactions were probably stopped. This may indicate that the X-ray burst had consumed almost all the nuclear fuel on the neutron star, and the stop of the time-dependent fusion reaction contributes to a significant part of the 7% X-ray flux decrease.

The inner disk radii before and after the X-ray burst, derived from Table 1, are about 300 and 360 km, respectively. For an accreting neutron star of 2.0 $M_\odot$, and taking $\cos(\theta) = 1$, the upper limits on the Keplerian frequencies corresponding to the two radii are 15 and 12 Hz. The spectral hardening would lead to an even larger inner disk radius and thus an even lower frequency (Shimura & Takahara 1995). On the other hand, the QPO frequency around 800 Hz is probably the lower of the twin peaks, which suggests that the Keplerian frequency at the inner edge of the disk should be around 1075 Hz (Zhang et al. 1998b). Thus, the derived inner disk radii are inconsistent with the beat-frequency model. The difference between the observed QPO frequency and those inferred from the spectral fit probably comes from a lack of detailed knowledge of the spectral components in neutron star X-ray binaries and the lack of sensitivity below 2 keV of the PCA to determine the parameters of a 0.26 keV blackbody spectral component. Conversely, it is also possible that the identification of the kHz QPOs as the Keplerian frequency at the inner edge of the accretion disk, or its beat frequency against the neutron star spin, is incorrect.

The observed QPO frequency decrease is 37 ± 5 Hz, which is about one-third of that inferred from the QPO frequency versus count rate relation. In principle, the decrease of the disk BB flux should originate from a decrease of the mass accretion rate. This would introduce a decrease of the QPO frequency. Taking the spectral parameters in Table 2 and using the PCA instrumental information, we estimate that the 2–10 keV PCA count rate of the disk BB is 23 ± 8 counts s^{-1} and that of the neutron star BB component is 47 ± 6 counts s^{-1}. So the QPO frequency decrease is consistent with the 23 counts s^{-1} count rate decrease of the disk BB component, which is about one-third of the total decrease of ~70 counts s^{-1}. Because the PCA effective area is not a constant with photon energy, and because the two BB components have quite different BB temperatures, the incident BB photon fluxes (Table 2) cannot replace the above count rate estimates when we study the frequency decrease inferred from the PCA count rate.

The central radiation force may also affect the QPO frequency. A decrease of the central BB emission from near the neutron star surface would probably introduce an increase of the QPO frequency. Thus, two mechanisms would account for the correlation between the QPO frequency and the count rate in Figure 2. One is that it is the disk BB flux instead of the total flux that is correlated with the QPO frequency. The QPO frequency variations between the data points on the right-hand side branch in Figure 2 originate from the disk BB flux variations. Thus, the data points in the lower left-hand corner may join in the data points of the right-hand side branch in a plot of the QPO frequency versus the disk BB flux. The other is that a decrease of the central BB radiation force after the X-ray burst would increase the QPO frequency, and then the QPO frequency did not follow the correlation relation when the central BB radiation force is nearly constant. Our study indicates that a comprehensive investigation of the correlation between QPO frequency and each spectral component is needed, especially when a flux decrease or spectral transition occurs.

We thank an anonymous referee for helpful comments and suggestions, which certainly improved this article. This work was supported by the National Natural Science Foundation of China under grants 19673010 and 19733003.

REFERENCES

Alpar, A., & Shaham, J. 1985, Nature, 316, 239
Bildsten, L. 1993, ApJ, 418, L21
Cui, W., et al. 1998, ApJ, 502, L49
Czerny, M., Czerny, B., & Grindlay, J. E. 1987, ApJ, 312, 122
Ford, E., et al. 1997, ApJ, 486, L47
Hasinger, G., & van der Klis, M. 1989, A&A, 225, 79
Kaaret, P., Ford, E. C., & Chen, K. 1997, ApJ, 480, L27
Kaaret, P., Yu, W., Ford, E. C., & Zhang, S. N. 1998, ApJ, 497, L93
Lamb, F. K., Miller, M. C., & Psaltis, D. 1998, preprint (astro-ph/9802348)
Lamb, F. K., Shibazaki, N., Alpar, M. A., & Shaham, J. 1985, Nature, 317, 681
Méndez, M., van der Klis, M., Ford, E. C., Wijnands, R., & van Paradijs, J. 1999, ApJL, in press (astro-ph/9811261)
Méndez, M., et al. 1998, ApJ, 494, L65
Miller, M. C., & Lamb, F. K. 1998, ApJ, 499, L37
Miller, M. C., Lamb, F. K., & Psaltis, D. 1998, ApJ, 508, 791
Mitsuda, K., et al. 1984, PASJ, 36, 741
Shimura, T., & Takahara, F. 1995, ApJ, 445, 780
Strohmayer, T., et al. 1996, ApJ, 469, L9
van der Klis, M. 1998, in Proc. Third William Fairbank Meeting, in press (astro-ph/9812395)
Verbunt, E., et al. 1994, A&A, 285, 903
Yu, W., et al. 1997, ApJ, 490, L153
Zhang, S. N., Yu, W., & Zhang, W. 1998a, ApJ, 494, L71
Zhang, W., Lapidus, I., White, N. E., & Titarchuk, L. 1996, ApJ, 469, L17
Zhang, W., et al. 1998b, ApJ, 495, L9
———. 1998c, ApJ, 500, L171